EXAMINATION OF TRANSPORT EQUATIONS PERTAINING TO PERMEABLE ELASTIC TUBULES SUCH AS HENLE'S LOOP

DIRAN BASMADJIAN, *Department of Chemical Engineering and Applied Chemistry, and*
ANDREW D. BAINES, *Department of Clinical Biochemistry, University of Toronto, Toronto, Ontario*

ABSTRACT The transport equations applicable to loops of Henle and similar elastic permeable tubules were re-examined to assess the effect of radial transport resistance in the lumen and tubule geometry on solute transport. Active transport at the wall as well as external gradients equivalent to a 2–1,000-fold concentration increase per centimeter of distance were considered. Wall permeabilities and active transport constants were varied up to $2 \cdot 10^{-2}$ cm/s. It is shown that for conditions applicable to the loop of Henle, resistance to radial solute transfer in the lumen is negligible, both for passive and active transmural transport with concomitant water flux, and that axial dispersion further reduces that resistance. These conclusions apply equally to conical and elliptical geometries likely to arise in loop operation. The validity of Poiseuille's equation for these geometries is discussed. It is concluded that the one-dimensional transport equations are a valid representation of loop operation.

INTRODUCTION

It is by now generally recognized that the concentrating mechanism in the loop of Henle is based on a combination of active and passive solute transport as well as water flux due to osmotic and possibly hydraulic driving forces. If one neglects any gradients in the radial direction, it is possible by simple one-dimensional mass balances to predict many of the qualitative features of loop function.

We recently undertook a detailed simulation study of loop function designed to reproduce more quantitatively observed water reabsorption, distal solute concentrations, transit times, and pressure drops.[1] In particular we wished to clarify the complex dependence of these variables on flow rate as observed in various microperfusion experiments (10, 12), and to interpret the results obtained when suction is applied to the distal end under conditions of constant inlet flow rate (1). Both velocity and luminal dimensions vary significantly in these experiments.

[1]Baines, A. D., D. Basmadjian, and B-C. Wang. 1978. Flow-dependent absorption in short Henle's loop. Three computer models compared to existent in vivo data. *And* Effects of lumen volume, transit time, and pressure on Henle's loop function. Submitted for publication.

Because of some puzzling features in the results, we initiated our study by a careful consideration of possible secondary effects, in particular the existence of significant radial solute gradients for various lumen geometries (cylindrical, conical, elliptical). If substantial enough, such gradients could result in a velocity-sensitive radial transport resistance and provide a tempting explanation for the observed velocity dependence of transmural transport.

Friedlander and Walser's analysis (6) of solute diffusion in the proximal tubule appears to be the only attempt so far to address this question quantitatively. They considered two simple asymptotic cases: (*a*) Diffusion of solute to a wall of constant concentration, (*b*) water flux with radial convection of solute and back diffusion in balance. In both these cases the liquid phase gradients were found to be negligible, but the authors stressed the desirability of extending their analysis to more realistic boundary conditions.

In the loop of Henle, wall concentrations can be expected to vary significantly in the direction of flow, in the descending thin limb (DTL) because of the very steep changes in peritubular concentrations, and in the ascending thick limb (ATL) because of continuous salt removal by active transport. Transmural water flux causes additional changes in the wall concentration. It then becomes entirely conceivable that substantial radial gradients will develop in the lumen, which will react to changes in velocity. Axial diffusion, itself velocity-sensitive, could also be expected to further modify the liquid phase resistance.

In what follows we shall estimate the liquid resistance to radial solute transport in different segments of the loop of Henle for various tubule geometries. We shall also briefly re-examine the validity of Poiseuille's law under conditions of substantial water reabsorption and deviation from cylindrical shape.

SYMBOLS AND ABBREVIATIONS

ATL Ascending limb of loop of Henle.

A_n Fourier coefficients.

B Cone parameter Vs_0^2/D, (m).

C Solute concentration (mol · m^{-3}).

C_m Mean cross-sectional concentration in tubule: $\int_0^R Cv\,2\pi r dr / \int_0^R v\,2\pi r dr$ (mol · m^{-3}).

C_w Solute concentration at tubule wall (mol · m^{-3}).

d Tubule diameter (circular) or hydraulic diameter = 4 × cross-sectional area/perimeter (ellipse) (m).

D Liquid phase diffusivity of solute (m^{2}s^{-1}).

DTL Descending thin limb of loop of Henle.

F Poiseuille law correction factor.

J_o, J_1 Zero and first-order Bessel functions of the first kind.

k_a Active transport rate constant (ms^{-1}).

k_L Solute mass transfer coefficient in liquid phase (m · s^{-1}).

k_w Solute mass transfer coefficient or permeability in tubule wall (ms^{-1}).

P Pressure (N m^{-2}).

Pe Peclet number, v_0R/D (dimensionless).

Q Volumetric flow rate (m^{3}s^{-1}).

r Radial distance in cylindrical tubule (m).
R Tubule radius (m).
R_h Hydraulic radius = 2 × cross-sectional area/perimeter (ellipse) (m).
s Radial distance in conical tubule (m).
s_0 Cone slant height (m).
Sh_L Liquid-phase Sherwood number, $k_L d/D$ (dimensionless).
Sh_w Wall Sherwood number, $k_w d/D$ (dimensionless).
u_w Radial water velocity at tubule wall ($m \cdot s^{-1}$).
v Fluid velocity ($m \cdot s^{-1}$).
v_0 Centerline fluid velocity ($m \cdot s^{-1}$).
V Average (linear) velocity ($m \cdot s^{-1}$).
x Axial distance (m).
y Dimensionless radial distance r/R (cylinder), or dimensionless angular distance ϕ/ϕ_0 (cone).
Y_n Eigenfunctions
z Dimensionless axial distance, $(x/R) \cdot (1/Pe)$.
β Dimensionless wall parameter, $k_a d/D$ (ATL) or $k_w d/D$ (DTL).
γ Exponential parameter expressing axial variation of peritubular concentration.
δ $\gamma \cdot R \cdot Pe$.
μ Viscosity ($N \cdot s \cdot m^{-2}$).
λ_n Eigenvalues.
ϕ Angular distance in cone.
ϕ_0 Cone apex half-angle.

Superscript

^{0} Conditions at tubule inlet.

ANALYSIS

Qualitative Aspects of Solute Transport in Tubular Flow

To provide a basis for the proper understanding of our analysis, we have sketched qualitative solute distributions for three different wall boundary conditions (Fig. 1). Concomitant water flux is not considered here but has, as shown later, only a minor distorting effect. Fig. 2 gives the results of existing mathematical solutions for some of the simpler wall conditions, expressed in terms of two dimensionless groups:

Liquid phase Sherwood number Sh_L

$$= \frac{\text{Liquid phase permeability} \times \text{lumen diameter}}{\text{Solute diffusivity}} = \frac{k_L \cdot d}{D}.$$

Dimensionless distance z

$$= \frac{\text{Axial distance}}{\text{Lumen radius}} \cdot \frac{\text{Solute diffusivity}}{\text{Centerline velocity} \times \text{lumen radius}} = \frac{x}{R} \cdot \frac{1}{Pe}$$

where Pe = Peclet number = $v_0 R/D$.

Here k_L is a liquid phase permeability or mass transfer coefficient which results from the replacement of the Fickian flux, $D \cdot (\partial C/\partial r)_w$ by the equivalent rate law $k_L(C_w - C_m)$, where C_m = mean cross-sectional concentration.

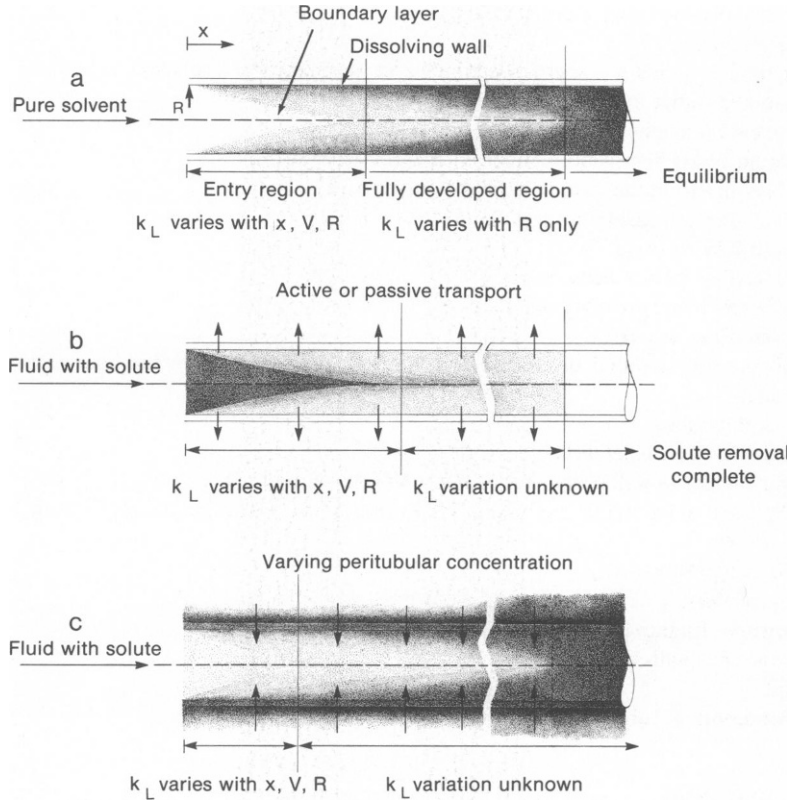

FIGURE 1 Concentration distributions in tubules under different wall boundary conditions. *a*. Constant concentration at the wall. *b*. Active or passive solute transport out of lumen (constant external concentration). *c*. Passive transport into lumen (varying external concentration).

All three cases shown in Fig. 1 exhibit an "entry-region," in which pronounced concentration gradients adjoin regions of essentially constant concentration, similar to the laminar sublayer ("unstirred layer") in turbulent flow near a wall. It is here that one finds the strongest dependence of k_L on velocity as well as distance (Fig. 2). Once the core of constant concentration is completely penetrated ("fully developed flow"), k_L becomes either constant (case 1*a*) or continues to vary with v_0 and x, although in a much less pronounced way (1*b*, 1*c*). Furthermore, even if the Sherwood number becomes constant, k_L will continue to vary inversely with lumen diameter.

We conclude from this that in the loop of Henle with its varying velocity and diameter, variable liquid phase permeabilities can, in principle, arise anywhere in the tubule for the different wall boundary conditions considered. Whether this is translated into a flow-dependent total transport coefficient, however, will depend on what fraction of the resistance resides in the liquid phase. This question is now taken up in more detail.

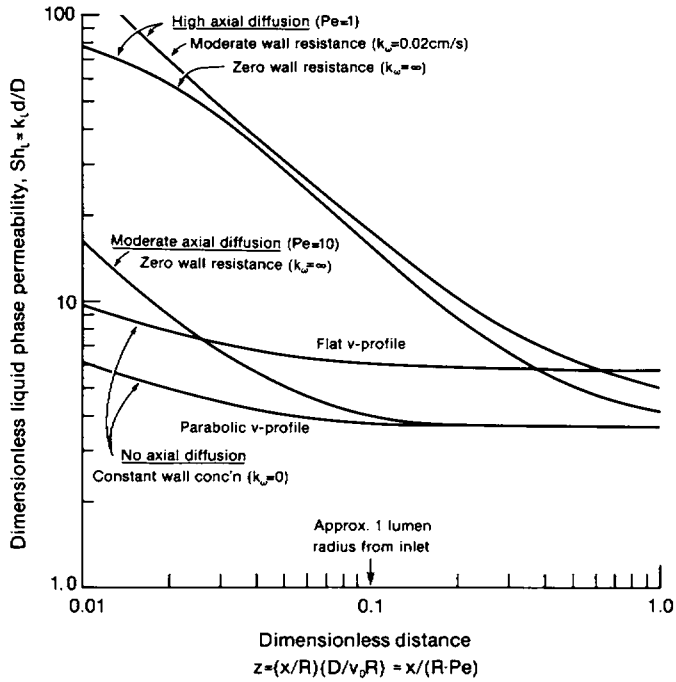

FIGURE 2 Effect of wall conditions and axial dispersion on liquid phase permeabilities k_L in cylindrical tubules. Constant external concentration and parabolic velocity profiles except where indicated. Adapted from Skelland (14) and Hsu (8).

Concentration Distributions in a Cylindrical Tubule With Active Wall Transport (ATL)

The case considered here represents conditions in the ATL in which the predominant mechanism is active salt transport. Although some water abstraction is also thought to occur, its omission is justified, since this leads to an overestimation of radial solute gradients. We make the further simplification of linearizing the Michaelis-Menten kinetics, which likewise results in exaggerated gradients, since it overestimates the rate of solute depletion at the wall. Axial diffusion is omitted but we shall show later that it does not alter our conclusions.

With these simplifications, the solute distributions are described by the following partial differential equation.

$$v(r)\frac{\partial C}{\partial x} = D\left(\frac{\partial^2 C}{\partial r^2} + \frac{1}{r}\frac{\partial C}{\partial r}\right) \tag{1}$$

where $v(r) = V$ for a flat velocity profile and $v(r) = 2V[1 - (r/R)^2]$ for a parabolic velocity profile. V is the linear velocity, equal to flow rate divided by luminal cross-section $Q/\pi R^2$.

The associated boundary conditions are as follows:

Symmetry: $\partial C/\partial r = 0 \quad$ at $r = 0, x \geq 0$ (2)

(or C = finite)

Inlet: $C = C^0 \quad$ at $x = 0, R \geq r \geq 0$ (3)

Wall: $-D\,\partial C/\partial r = k_a C$ (4)

The solution of this Graetz problem takes the form of a Fourier expansion:

$$C(y, z)/C^0 = \sum_{n=1}^{\infty} A_n Y_n(\lambda_n, y) \exp(-\lambda_n^2 z) \tag{5}$$

where Y_n and λ_n are the eigenfunctions and eigenvalues, y and z the dimensionless radial and axial distances.

For plug flow, a simple change of variables ($z \rightarrow t$, $D/V \rightarrow D'$) transforms the system to the classical diffusion equation with the solution (ref. 7, p. 73):

$$C(y, z)/C^0 = \sum_{n=1}^{\infty} \frac{2\beta}{(\lambda_n^2 + \beta^2)} \frac{J_0(\lambda_n y)}{J_0(\lambda_n)} \exp(-\lambda_n^2 z) \tag{6}$$

where the J_0's are zero-order Bessel functions of the first kind and the eigenvalues λ_n roots of $\lambda J_1(\lambda) = \beta J_0(\lambda)$, tabulated in Crank (5). The wall reaction rate is expressed through the dimensionless wall reaction number $\beta = dk_a/D$, which ranges in value from 2×10^{-3} to 2 for the case at hand.

The case of a fully developed velocity profile has been studied (for heat transfer) by Sideman et al. (13) and Hsu (8), but their tabulated coefficients do not extend below a value of $\beta = 4$. We have made use instead of the extensive but less accessible tabulations of Solomon and Hudson (15, 16), applicable to a tubular reactor with first-order reactions at the wall and in the fluid (the latter being omitted here).

TABLE I

VALUES OF A_n, Y_n AND λ_n

Wall Sherwood or active transport number β:	Plug velocity,* (cylindrical and conical tubes)				Parabolic velocity,‡ (cylindrical tubes)			
	$2\cdot10^{-3}$	$2\cdot10^{-2}$	$2\cdot10^{-1}$	$2\cdot0$	$2\cdot10^{-3}$	$2\cdot10^{-2}$	$2\cdot10^{-1}$	$2\cdot0$
Fourier A_1	1.0005	1.0025	1.024	1.205	1.0002	1.0029	1.028	1.2013
Coefficients A_2	−0.00034	−0.00337	−0.0334	−0.2902	−0.00040	−0.00402	−0.03901	−0.2929
Eigenvalues λ_1	0.0447	0.1412	0.4417	1.256	0.0632	0.1995	0.6183	1.641
λ_2	3.825	3.834	3.858	4.080	5.068	5.073	5.117	5.478
Eigenfunctions								
$Y_1(0), r = 0$	1.000	1.0000	1.0000	1.0000	1.0000	1.0000	1.0000	1.0000
$Y_1(1), r = R$	0.9995	0.9950	0.9518	0.6429	0.99925	0.9925	0.9295	0.5497
$Y_2(0), r = 0$	1.0000	1.0000	1.0000	1.0000	1.0000	1.0000	1.0000	1.0000
$Y_2(1), r = R$	−0.4027	−0.4027	−0.4026	−0.3907	−0.4925	−0.4918	−0.4847	−0.4080

*Calculations based on tabulations of Crank (5, pp. 73, 330).

‡Calculations based on tabulations of Solomon and Hudson (15, 16).

TABLE II

PHYSICAL PARAMETER VALUES USED IN THE ANALYSIS OF THE LOOP OF HENLE

Tubular radius, R	10^{-3} cm
Average fluid velocity, V	10^{-1} cm s^{-1}
Solute diffusivity, D	2.10^{-5} cm^2 s^{-1}
Fluid viscosity, μ	1 cp
Fluid density, ρ	1 g cm^{-3}
Wall permeability in DTL, k_w	$\leq 2.10^{-3}$ cm s^{-1}
Active transport constant in ATL, k_a	$\leq 2.10^{-2}$ cm s^{-1}
Axial Reynolds number, $Re = Rv_0\rho/\mu$	$1.10^{-2} - 2.10^{-2}$
Schmidt number, $Sc = \mu/\rho D$	5.10^2
Peclet number, $Pe = RV/D$ (plug flow)	5
$= dV/D$ (parabolic velocity)	10
Wall Sherwood number, $Sh_w = dk_w/D(=\beta)$	≤ 2
Wall reaction number, $Rn_w = dk_a/D(=\beta)$	≤ 2
Dimensionless axial distance, $z = x/(R \cdot Pe)$	
Plug flow:	50 × cm length
Parabolic velocity:	100 × cm length
Exponential factor for peritubular concentration, γ,	4.6
and $\delta = \gamma \cdot R \cdot Pe$	$4.6 \cdot 10^{-2}$ cm

The first two values for the coefficients A, λ, and Y calculated from the tabulations of Crank and Solomon are displayed in the Table I. Values for the eigenfunction Y are listed both for the centerline and wall positions. It can be verified from these numbers that convergence of the series (Eq. 5) is very rapid for tubule flow with the physical characteristics of the loop of Henle (Table II). At a distance of only one radius from the inlet, and using the most adverse conditions ($\beta = 2.0$, parabolic profile), the second term is less than 2% of the first. For all practical purposes, therefore, the series may be truncated after the first term. The ratio of wall to centerline concentration at any given axial location is then simply given by the value of the first eigenfunction at the wall:

$$[C_{r=R}/C_{r=0}]_{z=\text{constant}} = Y_1(1) = f(k_a d/D) \tag{7}$$

This expression was used to compute the concentration ratios shown in Table III, discussed more fully below.

Concentration Distribution in a Tubule with Varying External Concentration (DTL)

The major transport mechanisms in the DTL are generally thought to be water reabsorption by osmotic forces, and passive flow of solute into the lumen from an external medium with steep axial solute gradients. Here the radial convection can no longer be ignored, since it tends to aggravate solute gradients and a rigorous derivation of concentration profiles would confront us with a major computational effort. The results of Friedlander and Walser (6) showing only very minor gradients due to water flux alone (under admittedly milder conditions) led us to consider the diffusional

TABLE III

CALCULATED RATIOS OF WALL TO CENTERLINE CONCENTRATION IN LOOP OF HENLE-LIKE TUBULES

Wall permeability, k_w, or active transport constant k_a:	$\frac{2.10^{-5}\,cm\,s^{-1}}{(\beta = 2.10^{-3})}$	$\frac{2.10^{-4}\,cm\,s^{-1}}{(\beta = 2.10^{-2})}$	$\frac{2.10^{-3}\,cm\,s^{-1}}{(\beta = 2.10^{-1})}$	$\frac{2.10^{-2}\,cm\,s^{-1}}{(\beta = 2.0)}$
Ascending limb	$C_{wall}/C_{centerline}$			
Cylindrical tube, plug flow velocity	0.99950	0.9950	0.952	0.64
Cylindrical tube, parabolic velocity	0.99925	0.9925	0.930	0.55
Conical tube, plug flow velocity	0.99950	0.9950	0.952	0.64
Descending limb	$(C_{ext} - C_{wall})/(C_{ext} - C_{centerline})$ (=min. fractional wall resistance)			
(Cylindrical tube, parabolic velocity)				
Constant external concentration	0.99925	0.9925	0.930	0.55
Varying external concentration $C^{\circ}_{ext}\exp(4.6x)$	0.99925	0.9925	0.930	0.55

For axial distances over one lumen radius from inlet. Physical parameters used are listed in Table II. See text for effect of water reabsorption and axial diffusion.

process as a separate event, followed by an approximate assessment of the effect of concomitant water flux. For solute diffusion alone, the same Eqs. 1–3 apply, with the wall boundary condition now given by:

$$D\frac{\partial C}{\partial r} = k_w[C_{ext}(x) - C] \tag{8}$$

For C_{ext} we chose an exponential representation:

$$C_{ext}(x) = C^{\circ}_{ext}\exp(\gamma x) \tag{9}$$

where C°_{ext} and γ are arbitrarily adjustable parameters. γ values giving up to 1,000-fold increases in external concentration per centimeter of axial distance were considered.

To solve this case, we first note that for constant C_{ext}, Eq. 5 becomes:

$$\frac{C^{\circ}_{ext} - C}{C^{\circ}_{ext} - C^{\circ}} = \sum_{n=1}^{\infty} A_n Y_n(\lambda_n, y)\exp(-\lambda_n^2 z) \tag{10}$$

For variable concentrations one can apply the generalized convolution integral proposed by Bartels and Churchill (2) to Eq. 10, obtaining

$$C(y,z) = \frac{\partial}{\partial z}\int_0^z C^{\circ}_{ext}\exp(\delta z')dz' - \frac{\partial}{\partial z}\int_0^z (C^{\circ}_{ext}\exp(\delta z') - C^{\circ})\Sigma A_n Y_n \exp(-\lambda_n^2[z - z'])dz', \tag{11}$$

where $$C_{ext} = C^{\circ}_{ext} \exp(\gamma x) = C^{\circ}_{ext} \exp(\gamma \cdot R \cdot Pe \cdot z) = C^{\circ}_{ext} \exp(\delta z). \quad (12)$$

Evaluation of the integrals and some algebraic manipulation reduce Eq. 11 to the following series:

$$C^{\circ}_{ext} \exp(\delta z) - C(y,z) = C^{\circ}_{ext} \exp(\delta z) \sum_{n=1}^{\infty} \frac{A_n Y_n}{1 + \lambda_n^2/\delta} - \left(\sum_{n=1}^{\infty} C^{\circ} - \frac{C^{\circ}_{ext}}{1 + \delta/\lambda_n^2} \right) A_n Y_n \exp(-\lambda_n^2 z). \quad (13)$$

Here A_n, Y_n, and λ_n have the same values as those used in the analysis of the ascending limb and listed in Table I.

To test for convergence, we choose a value of $\gamma = 4.6$, corresponding to a 100-fold increase in peritubular concentration per centimeter axial distance. Using the same "worst case" conditions as before ($\beta = 2.0$, $x = R$, parabolic velocity profile), convergence is found to be at least as rapid as in the previous analysis. Equally rapid convergence is obtained for a 1,000-fold increase per centimeter. Truncating the series after the first term, one arrives at the equation

$$C^{\circ}_{ext} \exp(\delta z) - C(y,z) = \frac{A_1 Y_1}{1 + \lambda_1^2/\delta} C^{\circ}_{ext} \exp(\delta z) - \left[A_1 Y_1 C^{\circ} - \frac{C^{\circ}_{ext}}{1 + \delta/\lambda_1^2} \right] \exp(-\lambda_1^2 z). \quad (14)$$

For the wall to centerline concentration differences, this reduces to the simple expression

$$(C_{ext} - C_{r=R})/(C_{ext} - C_{r=0}) = Y_1(1) = f(k_w d/D) \quad (15)$$

Since $C_m \geq C_{r=0}$, this concentration ratio equals the minimum possible fractional wall resistance.

We have summarized the results for both ATL and DTL in terms of wall to centerline concentration ratios (Table III) and fractional resistance in the liquid phase (Table IV). Luminal radius and fluid velocity were held constant at values typical for the loop of Henle (Table II); changes in the variables over the physiological or experimental range do not affect the conclusions. The main parameters studied were k_w and k_a, which in the loop are of the order 10^{-5}–10^{-3} but were varied over the wider range of $2 \cdot 10^{-5}$–$2 \cdot 10^{-2}$ cm/s. The principal conclusion which emerges is that for wall permeabilities or active transport constants up to $2 \cdot 10^{-3}$ cm/s, the fluid phase resistance is negligible. At the highest value, $2 \cdot 10^{-2}$ cm/s, substantial gradients do arise, but the solute transfer is by now so rapid that the effect is limited to short distances from the inlet of the ATL or DTL. It is only in the range of $2 \cdot 10^{-3}$–$2 \cdot 10^{-2}$ cm/s that a significant effect may arise, since radial gradients are beginning to make themselves felt, but solute transfer at the wall is not yet quick enough for rapid equi-

TABLE IV

EFFECTIVE LIQUID PHASE RESISTANCE AS A PERCENTAGE OF TOTAL RADIAL TRANSPORT RESISTANCE IN LOOP OF HENLE-LIKE TUBULES*

Wall permeability, k_w, or active transport constant, k_a:	2.10^{-5} cm s^{-1} ($\beta = 2.10^{-3}$)	2.10^{-4} cm s^{-1} ($\beta = 2.10^{-2}$)	2.10^{-3} cm s^{-1} ($\beta = 2.10^{-1}$)	2.10^{-2} cm s^{-1} ($\beta = 2.0$)
Ascending limb	*% liquid phase resistance* $(1/k_L)/(1/k_L + 1/k_w)$ or $(1/k_L)/(1/k_L + 1/k_a)$			
Cylindrical tube, plug flow velocity	0.025%	0.25%	2.4%	21.2%
Cylindrical tube, parabolic velocity	0.044%	0.44%	4.4%	32.6%
Elliptical tube, fully developed velocity, aspect ratio 1.25†	—	—	4.5%	32.7%
Descending limb				
Cylindrical tube, parabolic velocity, constant C_{ext}	0.044%	0.44%	4.4%	32.6%
Cylindrical tube, parabolic velocity, varying C_{ext}		Liquid phase resistance varies with distance but is insignificant.		>32.6% but eq'm attained ~ 1R from inlet

*For axial distances over one lumen radius from inlet. Physical parameters used are listed in Table II. See text for effect of water flux and axial diffusion.

†From calculations of Schenk and Han (11).

libration or depletion to take place. However, this region is deemed to be well outside the range of normal loop parameters.

Effect of Water Reabsorption on Concentration Distributions in DTL

An estimate of this effect may be arrived at by a simple mass balance applied at the tubule wall:

$$k_w(C_{ext} - C_w) + u_w C_w = k_L(C_w - C_m) \qquad (16)$$

Solute reaching wall *Solute leaving wall,*

where u_w = radial water velocity at tubule wall, and the reflection coefficient has been set at 1, since this gives the maximum accumulation at the wall.

Rearrangement leads to the expression:

$$C_w/C_m = \frac{(k_w C_{ext}/k_L C_m) + 1}{1 + k_w/k_L - u_w/k_L}. \qquad (17)$$

For water reabsorption to have a noticeable effect on radial solute gradients, u_w/k_L would have to be of the order 10^{-1} or greater. An estimate of u_w may be obtained from the water reabsorption data reported by Morgan and Berliner (10), as in that of Friedlander and Walser (6). Using the maximum value given in ref. 12, 10 nl/min, and assuming as a "worst case" that all reabsorption takes place in the DTL with dimensions $R = 10\,\mu$m, $L = 0.15$ cm, we arrive at a value

$$u_w = \frac{Q}{2\pi RL} = \frac{10 \times 10^{-7}/60}{2\pi \times 10 \times 10^{-4} \times 0.15} = 1.65 \times 10^{-4}\,\text{cm/s}. \qquad (18)$$

For k_L we use the values obtained in the absence of water flux (Table IV), noting that these are conservative, since any enhanced polarization due to the radial convection would tend to increase k_L, much as in the entrance regions of the tubules.

Using these values, one obtains:

k_w	k_w/k_L	u_w/k_L
cm/s		
2×10^{-5}	4×10^{-4}	3.3×10^{-3}
2×10^{-4}	4×10^{-3}	3.3×10^{-3}

Examination of Eq. 17 shows that u_w/k_L will lower C_w/C_m by no more than about 0.3%, and we conclude from this that the net concentration polarization due to water flux is negligible.

Axial Diffusion Effects

At sufficiently low flow rates, axial diffusion in the lumen may become large enough to require its inclusion in the solute mass balances. In the usual one-dimensional models this is done by adding an appropriate second-order term to the balance. Before one can safely use this procedure, however, it is necessary to consider the effect of axial diffusion on the liquid phase permeability k_L.

Inclusion of axial diffusion in the two-dimensional model (Eq. 1) complicates its solution considerably, and the literature contains only limited treatments of this case for cylindrical tubules with constant external conditions. These are sufficient, however, to establish important qualitative trends. We have used the results of an analysis by Hsu (8) of the equivalent heat transfer case, covering the range $k_w = 2.10^{-2}$–2 cm/s ($\beta = 4 - 400$), the higher value being virtually identical to "no wall resistance." Some of his computed liquid phase transfer coefficients have been recast into Sherwood numbers and are reproduced in Fig. 2.

Several important trends can be discerned in these plots. One is that axial diffusion considerably increases the entry length, but at the same time the liquid phase coefficient k_L increases by orders of magnitude over the values obtained for zero axial diffusion. When a wall resistance is included, these effects are even more pronounced. Although we do not have the results for k_w values applicable to the loop of Henle, this trend indicates that axial diffusion will result in a net increase of the liquid phase permeability, leading to an even greater predominance of wall resistance or reaction rate.

Solute Transfer in Noncylindrical Tubules

The most likely tubule geometries to result from changes in transmural pressures are the tapering circular and elliptical shapes. The solution even of the classical Graetz problem becomes fairly complex for these geometries. We have limited ourselves to the

consideration of two simple yet useful cases for which some supporting material was available in the literature:

(*a*) Plug flow in a convergent cone with small apex half angle ($\phi_0 \leq 0.1$); (*b*) Fully developed laminar flow in an elliptical tube of constant perimeter and aspect ratio (major to minor axis) of 1.25.

For the cone, we extended the treatment of Cobble (4) for heat transfer with constant wall temperatures to our case of a first-order wall reaction (ATL) and passive transport from a medium with C_{ext} = constant. The operative equation is:

$$(B - 2s)\frac{\partial C}{\partial s} = \frac{\partial^2 C}{\partial s^2} + \frac{1}{\phi}\frac{\partial C}{\partial \phi}, \tag{19}$$

with boundary conditions:

Symmetry: $$C = \text{finite at } \phi = 0, s_0 \geq s > 0; \tag{20}$$

Inlet: $$C = C^\circ \quad \text{at } s = s_0, \phi_0 > \phi > 0; \tag{21}$$

Wall: $$-D\frac{\partial C}{\partial \phi} = k_a C \quad \text{at } \phi = \phi_0, s_0 \geq s \geq 0 \tag{22}$$

or $$D\frac{\partial C}{\partial \phi} = k_w(C_{ext} - C).$$

where $B = Vs_0^2/D$ and ϕ, s depict the geometry of the cone (Fig. 3).

By a separation of variables procedure one obtains, for active transport:

$$\frac{C(s,y)}{C^\circ} = \sum_{n=1}^{\infty} \frac{(2\beta J_0(\lambda_n y))}{(\lambda_n^2 + \beta^2) J_0(\lambda_n)} \left[\frac{B + 2s}{B + 2s_0}\right]^{1/2(\lambda_n/\phi_0)^2}. \tag{23}$$

For passive transport, the left side is replaced by $(C_{ext} - C)/(C_{ext} - C^\circ)$. The eigenvalues λ_n are in both cases the same as those for the cylindrical tube with plug flow.

For the rather extreme case of a conical tubule closed at the tip and of slant height $s_0 = 0.5$ cm, one obtains, using the physical characteristics listed in Table II, $\phi_0 = 2.10^{-3}$, $B = 1.25 \cdot 10^3$ cm.

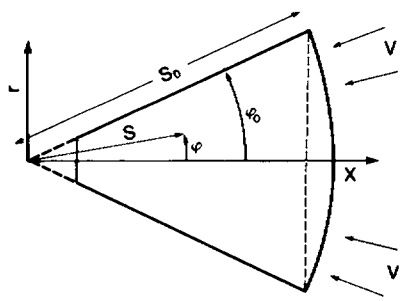

FIGURE 3 Coordinate system for flow in conical tubules.

It can again be shown using the coefficients in Table I that the series can be truncated after the first term, so that the wall to centerline concentration ratio becomes:

$$\left[\frac{C_{\phi=\phi 0}}{C_{\phi=0}}\right]_{s=\text{constant}} = Y_1(1). \tag{24}$$

Since the centerline position of the arc s = constant is only $\sim 10^{-6}$ cm removed from that of the cord, Eq. 24 is equivalent to the expression

$$[C_{r=R}/C_{r=0}]_{z=\text{constant}} = Y_1(1). \tag{25}$$

It is relatively simple to extend this solution to the case of varying peritubular concentrations, as was done before. In view of the close similarity in the behavior of conical and cylindrical tubules, the solution given for the latter case was considered sufficient for our purposes.

For the elliptical conduit, no attempt was made to derive detailed profiles; instead, we used the equivalent Sherwood numbers computed by Schenk and Han (11) for wall permeabilities of 2.10^{-3} and 2.10^{-2} cm/s and an aspect ratio of 1.25. The results are very close to those obtained for cylindrical tubules (Table IV). For a higher aspect ratio of 4, computed values are available only for the case of constant wall conditions. They indicate that k_L values will be marginally higher than those applicable to the cylindrical tubule (11). Variable wall conditions can be expected to raise k_L even further, so that liquid phase resistance can be considered negligible even for highly elliptic geometries.

Equations for Frictional Pressure Drop along Tubules

A complete model for solute and water transfer in an elastic tubule must include the hydrodynamic pressure drop, since it affects lumen radius and the rate of transmural transport. Deviations from Poiseuille's law, commonly used for this purpose, can arise as a result of two factors: distortion of the velocity profile due to radial water transport and due to changes in the tubule geometry. A study of the former was recently carried out by Marshall and Trowbridge (9). Using their results for our maximum water flux (Eq. 18), we found the deviation from Poiseuille's law to be less than 0.1%. Similar conclusions are reported by Bossert and Schwartz (3).

To calculate pressure drops in noncircular conduits, it is customary to replace R in Poiseuille's equation by an equivalent cylindrical radius ("hydraulic radius") R_h = 2 × cross-sectional area/perimeter. An additional correction factor F is applied to bring the equation in line with the rigorous hydrodynamic solutions:

$$dP/dx = -F(8\mu Q/\pi R_h^4). \tag{26}$$

Results given by White (17, p. 130) show that for elliptical conduits with aspect ratios of 2, 4, and 10, the discrepancy between approximate and rigorous equivalent radii is respectively +3, 7, and 10%. The corresponding correction factors F are then 1.12, 1.31, and 1.48. It follows that the use of R_h and an uncorrected Poiseuille equation would lead to a significant underestimation of the pressure drop at high degrees of

ellipticity. To keep this finding in proper perspective, however, it should be kept in mind that the kidney tubule could not plausibly exceed an aspect ratio of 4 without collapse and that the observed tubule radii themselves are unlikely to be more than 10% accurate. The uncertainty attached to the use of the uncorrected Poiseuille equation for elliptical forms is thus less than that of the physical parameters used in the model equations.

To investigate the effect of a conical geometry, we have drawn on the rigorous analysis of Happel and Brenner (7) for laminar flow in converging and diverging circular conduits. They show that for small values of the apex half angle ($\phi_0 \leq 0.1$), the frictional pressure drop can be expressed as

$$dP/ds = -8\mu Q/\pi(s\phi_0)^4 \tag{27}$$

where s = slant height (see Fig. 3).

For a conical tubule 0.5 cm long and closed at the tip, ϕ_0 is of the order of 10^{-3}. If we consider the even more extreme case, $\phi_0 = 10^{-1}$, we obtain

$$s = x/\cos\phi_0 \simeq x/(1 - 5.10^{-3}), \tag{28}$$

$$(s\phi_0)^4 = (R\phi_0/\sin\phi_0)^4 \simeq R^4/(1 - 2.67 \cdot 10^{-2}). \tag{29}$$

or an equivalent correction factor F to Poiseuille's law of ~ 0.98.

Conclusions

We have shown that in normal operation of loop of Henle and similar tubules, the resistance to transmural water and solute flux resides entirely in the wall and is unaffected by axial velocity and lumen shape except where these variables cause a change in wall thickness. Deviations from Poiseuille's law for noncylindrical shapes are either insignificant (conical tubules) or of a magnitude similar to the uncertainty in measured tubule radii (elliptical tubules). The one-dimensional model equations can be considered a valid representation of loop function.

We wish to thank I. Danyliuk, who contributed significantly to the early stages of this work.

Received for publication 15 March 1978 and in revised form 6 June 1978.

REFERENCES

1. BAINES, A. D. and D. K. WU. 1974. Physical factors influencing fluid reabsorption from Henle's loop. *Can. J. Physiol. Pharamacol.* **53**:224–230.
2. BARTELS, R. C. F., and R. V. CHURCHILL. 1942. Resolution of boundary problems with the use of a generalized convolution. *Bull. Am. Math. Soc.*, **48**:276–282.
3. BOSSERT, W. H., and W. B. SCHWARTZ. 1967. Relation of pressure and flow to control of sodium reabsorption in the proximal tubule. *Am. J. Physiol.* **213**:793–802.
4. COBBLE, M. H. 1962. Nusselt number for flow in a cone. *J. Heat Transfer.* **84**:264–265.
5. CRANK, J. 1956. The Mathematics of Diffusion. Oxford University Press, London, England. 73, 330.
6. FRIEDLANDER, S. K., and M. WALSER. 1965. Some aspects of flow and diffusion in the proximal tubule of the kidney. *J. Theor. Biol.* **8**:87–96.
7. HAPPEL, J. and H. BRENNER. 1973. Low Reynolds Number Hydro-Dynamics. 2nd edition. Noordhoff International Publishing, Leyden, The Netherlands. 139.

8. HSU, C-J. 1968. Exact solution to entry-region laminar heat transfer with axial conduction and the boundary condition of the third kind. *Chem. Eng. Sci.* **23**:457–468.
9. MARSHALL, E. A., and E. A. TROWBRIDGE. 1974. Flow of a Newtonian fluid through a permeable tube. The application to the proximal renal tubule. *Bull. Math. Biol.* **36**:457–475.
10. MORGAN, T., and R. W. BERLINER. 1969. A study by continuous microperfusion of water and electrolyte movements in the loop of Henle and distal tubule of the rat. *Nephron.* **6**:388–405.
11. SCHENK, J., and B. S. HAN. 1967. Heat transfer from laminar flow in ducts with elliptical cross-section. *Appl. Sci. Res.* **17**:96–114.
12. SCHNERMANN, J. 1968. Microperfusion study of single short loops of Henle in rat kidney. *Pflügers Archiv Gesamte. Physiol. Menschen Tiere.* **300**:255–282.
13. SIDEMAN, S., D. LUSS, and R. E. PECK. 1964. Heat transfer in laminar flow in circular and flat conduits with (constant) surface resistance. *Appl. Sci. Res.* **A14**:157.
14. SKELLAND, A. H. P. 1974. Diffusional Mass Transfer. John Wiley & Sons, Inc., New York. 137.
15. SOLOMON, R. L. 1967. Solution of problems of transport with reaction by orthogonalization methods. M.Sc. thesis, University of Illinois at Urbana. See also Document No. 9311, American Documentation Institute, Library of Congress, Washington, D.C.
16. SOLOMON, R. L., and J. L. HUDSON. 1967. Heterogeneous and homogeneous reactions in a tubular reactor. *Am. Inst. Chem. Eng. J.* **13**:545–550.
17. WHITE, F. M. 1974. Viscous Fluid Flow. McGraw-Hill Book Company, New York. 130.